

Large-scale tribological characterisation of eco-friendly basalt and jute fibre reinforced thermoset composites

Levente Ferenc Tóth^{1,2}, Jacob Sukumaran¹, Gábor Szebényi², Ádám Kalácska¹, Dieter Fauconnier^{1,3}, Rajini Nagarajan⁴, Patrick De Baets^{1,5}

¹ Soete Laboratory, Department of Electrical Energy, Metals, Mechanical Constructions and Systems, Ghent University, Technologiepark Zwijnaarde 46, B-9052 Zwijnaarde, Belgium.

² Department of Polymer Engineering, Faculty of Mechanical Engineering, Budapest University of Technology and Economics, Műegyetem rkp. 3, H-1111 Budapest, Hungary

³ FlandersMake@UGent – Core lab EEDT-MP

⁴ Centre for Composite Materials, Department of Mechanical Engineering, Kalasalingam University, Krishnankoil, Tamilnadu, 626126, India

⁵ FlandersMake@UGent – Core lab EEDT-DC

Abstract

The present research aims at understanding the tribological behaviour of advanced unsaturated polyester/vinyl ester based thermoset composites reinforced by inorganic (mineral-based) or organic (vegetal) fibres such as basalt and jute. These fibres are non-toxic and widely available in nature. Thermosets have limitations in the formation of a uniform transfer layer during sliding wear. To surpass these limitations, tribo-fillers such as polytetrafluoroethylene, polyoxymethylene or molybdenum disulphide (PTFE/POM/MoS₂) are added into the contact surface. The composites developed for the current research are characterised for their friction and wear behaviour, using a large-scale (sample size typically 50 x 50 x 7 mm) linear reciprocating sliding flat-on-flat test configuration. In order to simulate real scale application, 50 mm/s sliding speed and 10 kN normal force which corresponds to 4 MPa contact pressure, are applied under dry contact conditions. In this research work 12 different tribocomposites are developed and tested against AISI 100Cr6 steel counterface. It was evidenced that composites blended with PTFE have the lowest coefficient of friction and longest service life. MoS₂ filled tribocomposites have the highest coefficient of friction. The dominant wear mechanisms for the failure of all investigated composites are thermal degradation and delamination, and abrasion for the counter surface.

Keywords: polymer-matrix composite, thermosets, natural reinforcement, sliding wear, solid lubricants, transfer layer

1. Introduction

Polymers are widely used in large scale applications such as bearings, linear slides, gears or guideways under both dry and lubricated conditions [1-4]. Semi-crystalline thermoplastics, such as e.g. polyoxymethylene (POM), polyether ether ketone (PEEK), polyamide 6 (PA6) and polytetrafluoroethylene (PTFE) are beneficial due to their ability to form an adequate transfer layer with uniform thickness on the counter surface [5-8]. This transfer layer can significantly improve the coefficient of friction and wear resistance on the condition that there is not too high adhesion between the formed transfer layer and the polymer sample [9]. Thermosets have some other advantages: they can withstand heavy loads and shock loading and they have a

good creep resistance [10]. Due to these features thermosets are frequently used as sliding bearing materials in heavy duty applications. But their tribological characteristics are inferior to thermoplastic materials, because their cross-linked molecular structure impedes formation of a uniform and durable transfer layer. The unfavourable tribological characteristics generally result into a higher coefficient of friction, higher frictional heating and consequently decreased service life [11]. To provide a protective transfer layer, functional additives are inserted. PTFE, graphite or molybdenum disulphide (MoS_2) can act as a solid lubricating agent [12, 13]. Lower coefficient of friction of graphite and MoS_2 are attributed to their lamellar structure. The lubricating action of PTFE is caused by the slip between the long molecular chains of this material. Sometimes tribo-fillers in particle form are also added and blended with the base/matrix material. Apart from blending, the contact surfaces can also be coated with tribo-fillers [14].

In the recent years, several attempts were made to incorporate natural (fibrous) materials into tribocomposites [15-17], because of their non-toxic nature. Being available in nature they can be considered of renewable resource [18]. With these fibres relatively high mechanical properties can be achieved with a lower environmental footprint [19, 20]. The relatively high fibre strength and low density of natural fibres are e.g. used in automotive industry [15, 20]. Compared to vegetal natural fibres, the mineral-based basalt fibre has higher elastic modulus and tensile strength [21]. The volcanic originated raw base material of the basalt fibre can be cheaply extracted [22]. Basalt fibre can also compete and surpass glass fibres in polymer matrices, due to its good and uniform strength characteristics [21-25]. In practice the properties of basalt fibres are in between the two commonly used glass fibre properties (E and S type composition). The tensile strength and Young's modulus of basalt are in the same range as for glass fibres. Basalt is more resistant to alkali than glass fibre, but on the other hand glass fibres are more resistant to strong acids [21, 22]. The most advantageous properties of basalt include excellent electric insulator property and low moisture absorption [22]. Furthermore basalt is an environment friendly and biologically inert material [24, 26]. Due to its good heat stability and chemical resistance [22, 25] it may even overclass carbon fibres, especially where the carbon fibre reinforcement would make the structure too rigid or too expensive. Hybrid reinforcement of basalt and carbon fibre is also a potential alternative to develop fibre reinforced composites [27]. Its melting point at approximately $1580\text{ }^\circ\text{C}$ also allows basalt to be used for high temperature applications [22, 24]. Basalt is also a suitable material to be applied in concrete, as it has a good resistance against alkaline and acids [21].

Jute is a vegetal fibre, which is provided mainly from India, China and Bangladesh [28, 29]. Jute fibres are biodegradable and recyclable, and are composed of cellulose units [28]. Jute, compared to other vegetal natural fibres, has relatively high tensile strength, high production volume and is available at affordable cost [15, 30]. This environmentally friendly material also has good insulating properties for both of thermal and acoustic energy [31, 32]. The main challenge with vegetal natural fibres, however, is the large variation in properties, which can be flattened by control of the fibres origin and environment [33]. To reach a sufficient adhesion between the vegetal fibres and polymer-based matrix material different surface treatment methods can be used [34].

The present research aims at understanding the tribological behaviour of unsaturated polyester/vinyl ester based basalt/jute fibre reinforced composites with PTFE/POM/ MoS_2 tribo-fillers. These tribo-fillers are incorporated only in the matrix of the top layer. This top layer includes only one basalt or jute reinforcement layer which results a thickness of around 1 mm. With this configuration the mechanical properties at the bulk material can be kept at the original

level. The transfer layer formed on the counter surface was also investigated as a function of the applied tribo-fillers.

2. Experimental procedure

2.1. Test materials and mechanical characterisation

In this research work twelve different polymer tribocomposites were investigated. They were produced by hand lay-up technique at the Centre for Composite Materials, Kalasalingam University (India). The basalt and jute fabrics were impregnated with resin/curing agent mixture and stacked on each other until reaching the required thickness. Wax was used as a release agent. The laminated composites were compressed by means of dead weights, subsequently cured at room temperature (32 °C) for 24 h and finally post-cured at 70 °C for 3 hours in hot air oven. No further operations were performed on the contact surface of the specimens. All samples for mechanical and tribological tests were cut out by water jet machining.

The structure of these composites can be divided into two parts: the bulk material and the top layer, both including fibre reinforcement (textile) layers. This material combination was developed based on the experience from an initial investigation [35]. The bulk material has a purely mechanical role, while the top layer that is in contact with the counterface during wear testing, fulfils mainly a tribological role. Consequently, only the top layer should contain tribo-fillers. The bulk material does not include these tribo-fillers and as such does not suffer potential negative influence of these lubricants on its mechanical properties. The thickness of the tribological top layer corresponds to the thickness of one applied reinforcement layer, which is around 1 mm.

The composites developed in the present research work are divided into four different composite systems (see Table 1). The matrix material is unsaturated polyester (UPE) or vinyl ester (VE) resin, which was reinforced with basalt (B) or jute (J) textile layers. The tribo-fillers were PTFE, POM and MoS₂ in 2 or 4 wt% filler content. This range of filler contents is based on literature survey and is expected to be sufficient to promote adequate transfer layer formation. Higher tribo-filler content was not considered because it could reduce the mechanical properties significantly; e.g. 7.5 wt% of PTFE can reduce the compressive strength of epoxy composites with 21%, while 12.5 wt% leads to 37% strength reduction [36]. Similar tendency was reported for the hardness [36]. The tribo-fillers were added only to the top layer. The fibre content of basalt was chosen 40 to 45 wt% and of jute between 25 to 30 wt%. Both unsaturated polyester and vinyl ester thermoset matrices and the different tribo-fillers (PTFE, POM and MoS₂) were ordered from Sigma Aldrich Ltd., Bangalore, India. For the curing purpose, both Methyl Ethyl Ketone Peroxide (MEKP) and cobalt naphthenate were used as catalyst and accelerator, respectively. The basalt and jute reinforcement were purchased from Nickunj Eximp Entp Ltd., Chennai, India.

Tensile and flexural tests were performed on the tribocomposites according to ASTM-D 3039 and ASTM-D 790 standards using an Instron 3382 universal testing machine. All tests were performed at room temperature with 5 mm/min cross-head speed. Specimen geometry of 200 x 20 x 3 (mm) was used for tensile tests with a grip distance of 50 mm, and 127 x 12.7 x 3 (mm) geometry for flexural tests with a 90 mm of span distance. The hardness was measured with a Zwick H04.3150.000 digital hardness tester in Shore-D measurement range. The mean and standard deviation values were calculated from at least 5 measurements.

Table 1. Natural fibre reinforced polymer tribocomposites.

Material code	Resin	Fibre reinforcement	Tribo-filler
UPE/B/PTFE/2	Unsaturated polyester	Basalt	PTFE, 2 wt%
UPE/B/POM/2	Unsaturated polyester	Basalt	POM, 2 wt%
UPE/B/MoS ₂ /2	Unsaturated polyester	Basalt	MoS ₂ , 2 wt%
UPE/B/PTFE/4	Unsaturated polyester	Basalt	PTFE, 4 wt%
UPE/B/POM/4	Unsaturated polyester	Basalt	POM, 4 wt%
UPE/B/MoS ₂ /4	Unsaturated polyester	Basalt	MoS ₂ , 4 wt%
UPE/J/PTFE/2	Unsaturated polyester	Jute	PTFE, 2 wt%
UPE/J/POM/2	Unsaturated polyester	Jute	POM, 2 wt%
UPE/J/MoS ₂ /2	Unsaturated polyester	Jute	MoS ₂ , 2 wt%
VE/B/PTFE/4	Vinyl ester	Basalt	PTFE, 4 wt%
VE/B/POM/4	Vinyl ester	Basalt	POM, 4 wt%
VE/B/MoS ₂ /4	Vinyl ester	Basalt	MoS ₂ , 4 wt%

2.2. Tribological characterisation

The polymer tribocomposites were tribologically characterized by means of a large-scale linear reciprocating sliding flat-on-flat tribotester with dry contact condition. Figure 1 shows the heart of the tribotester. A central support block at two sides houses the metal counterfaces. The two polymer samples, fixed in appropriate holders, are pressed against the sliding block that moves up and down. A significant benefit of this equipment is that its size is close to real application. More detailed information of this equipment can be found in a previous publication [37].

The 100Cr6 steel counterfaces were polished to 0.2 μm Ra roughness value. The counterface size was 200 x 80 x 20 mm, while the size of the polymer samples was 50 x 50 x 7 mm. Wear tests were performed in a conditioning chamber which maintains a uniform 23 °C temperature and 50% relative humidity (RH). The bulk temperature resulting from frictional heating was measured with thermocouples which are placed in the steel counterface and located at 10 mm distance from the contact surface.

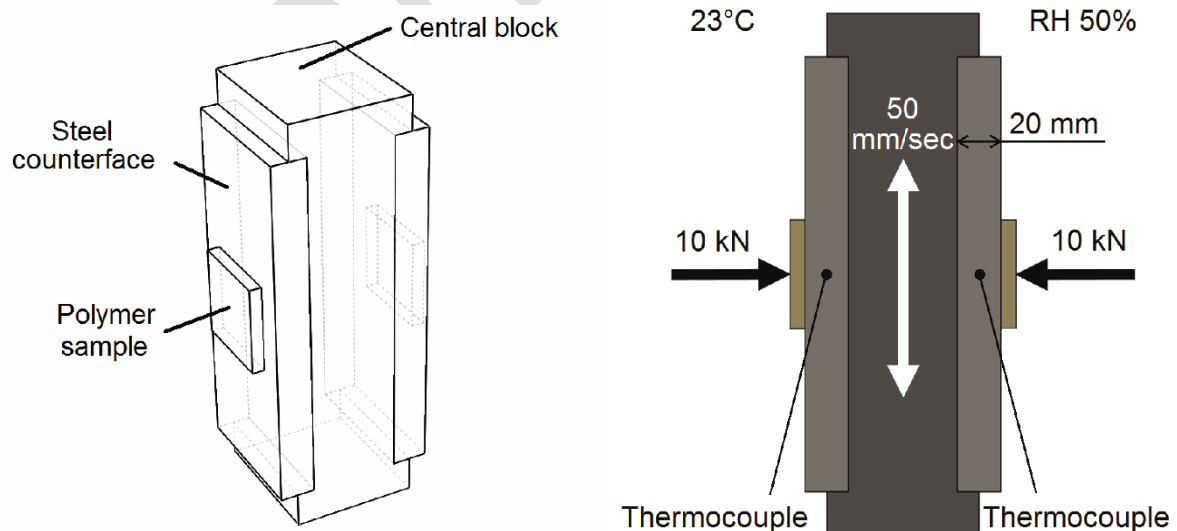


Figure 1. Schematic representation of reciprocating flat-on-flat tribotester

Considering heavy duty applications, all specimens were tested with 10 kN normal force, which corresponds to 4 MPa average contact pressure. The applied sliding speed was set to 50 mm/s, the stroke was 100 mm and the stipulated sliding distance was 5000 cycles

(corresponding to 1000 m). Independent tests were performed at least three times under identical test conditions to study the uncertainty from the tribotester where a deviation ($\pm 1\sigma$) of 10% in coefficient of friction and 20% in wear rate was observed. The online recording was provided with the use of NI 6036E DAQ (National instruments BNC 2100) in a LabVIEW platform. Data are sampled at a frequency of 500 Hz.

The static and dynamic coefficient of friction are derived from the results of every logged friction cycle. A typical cycle is shown in Figure 2. The sign switch of the force halfway the cycle indicates the reversal of the sliding motion direction. The maximum of the absolute values in the first and second stroke length are defined as the static coefficient of friction. The dynamic coefficient of friction is the average value of the centre (red marked) region in each stroke. The coefficient of friction is calculated with the following equation:

$$\mu = \frac{F_{Fr}}{2 \cdot F_N} \quad (1)$$

μ symbolises the calculated coefficient of friction [-], F_{Fr} is the measured friction force [N] and F_N is the applied normal force [N]. The factor 2 in this equation is needed to take into account the two friction faces.

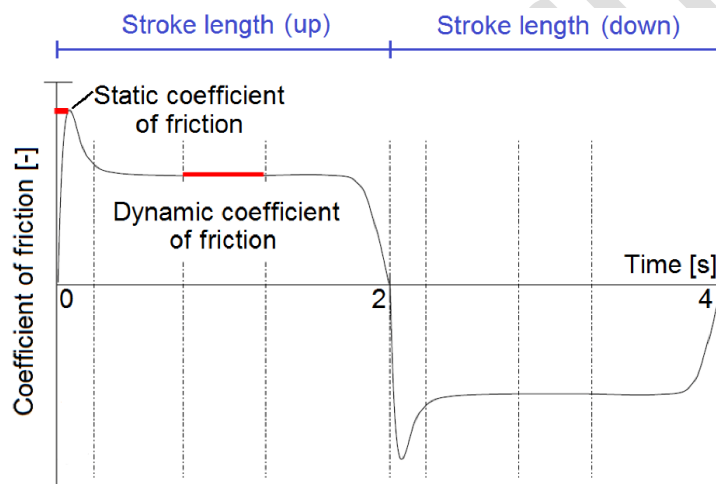


Figure 2. Friction cycle measured during reciprocating tribotesting

To calculate the average friction values, first the static and dynamic coefficient of friction were evaluated in every stroke (half cycle) as shown in Figure 2. The average static and dynamic coefficient of friction values are calculated at an interval between 20% and 80% of the lifetime (number of cycles). The reason of this method is that some of the materials did not reach steady state friction as they failed after a low number of cycles. By defining an interval between 20% and 80% of the lifetime, the effect of the initial and end period are minimised and the materials can be compared in a more precise way. Figure 3 shows an example of a friction curve with this interval indicated.

The surface roughness of the steel counter surface was scanned before and after wear testing by means of stylus profilometer (Surfscan 3D roughness tester, Hommel somiconic) with a stylus S6T (radius 2 μm , angle 90°). The average values and the standard deviations were calculated from 5 roughness measurements per sample. The measured roughness values were evaluated according to ISO 4288 standard with an assessment length $l_t = 4.00$ mm and cut-off wavelength $\lambda_c = 0.80$ mm for $0.1 \mu\text{m} < Ra \leq 2 \mu\text{m}$.

For the micrographs an Olympus reflected light bright field optical microscope was used. The image acquisition parameters were kept constant (150 μs exposure time and 30% illumination) for monitoring the transfer layer deposition.

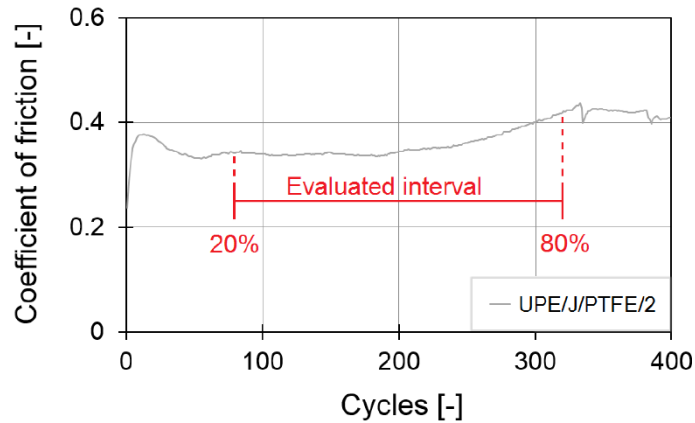


Figure 3. Example of friction curve (UPE/J/PTFE/2). AISI 100Cr6 steel counterface, 4 MPa contact pressure, 50 mm/s sliding speed, 100 mm stroke.

3. Results and discussion

3.1. Mechanical properties of the tribocomposites

The results of the static mechanical and hardness tests are shown in Table 2. Jute fibre reinforced composites had slightly lower hardness compared to basalt composites with the same 2 wt% tribo-filler content. The highest strength values were reached with the vinyl ester matrix. Jute fibre reinforcement results into significantly lower tensile and flexural strength compared to basalt fibres. This remarkable difference comes from the mechanical properties of jute and basalt fibres. The tensile strength and elastic modulus of jute fibre are 0.3-0.7 GPa and ~26 GPa, while for basalt fibre these values are ~2.8 GPa and ~89 GPa, respectively [21]. Significant difference in tensile and flexural strength was not registered as a function of the applied tribo-fillers. The measured differences were at the range of the standard deviation comparing PTFE, POM and MoS₂ fillers. It means that focusing on the tensile and flexural strength of the composites all tribo-fillers show similar performance. This indicates that in mechanical viewpoint all PTFE, POM and MoS₂ can be used with the same expectations on the mechanical strength in these composites as tribo-fillers.

Table 2. Mechanical properties of polyester and vinyl ester based tribocomposites. All deviations are related to $\pm 1\sigma$.

Materials	Tensile strength [MPa]	Flexural strength [MPa]	Hardness Shore-D
UPE/B/PTFE/2	152.9 ± 6.1	92.5 ± 4.6	82 ± 2.05
UPE/B/POM/2	150.4 ± 7.5	94.4 ± 3.7	80 ± 2.00
UPE/B/MoS ₂ /2	148.6 ± 4.5	95.9 ± 2.8	84 ± 2.10
UPE/B/PTFE/4	156.2 ± 7.8	96.2 ± 4.3	81 ± 2.03
UPE/B/POM/4	152.5 ± 3.8	93.5 ± 3.5	74 ± 1.85
UPE/B/MoS ₂ /4	150.4 ± 8.3	92.2 ± 2.1	79 ± 1.98
UPE/J/PTFE/2	29.1 ± 2.3	23.4 ± 1.2	76 ± 1.90
UPE/J/POM/2	28.4 ± 1.2	31.4 ± 0.9	73 ± 1.14
UPE/J/MoS ₂ /2	26.3 ± 1.8	32.5 ± 2.4	75 ± 1.88
VE/B/PTFE/4	329.1 ± 16.4	149.9 ± 4.1	82 ± 2.05
VE/B/POM/4	332.2 ± 15.4	151.3 ± 3.6	78 ± 1.95
VE/B/MoS ₂ /4	327.1 ± 12.8	148.6 ± 2.8	85 ± 2.13

3.2. Lifetime and coefficient of friction

The operational variables during wear testing were kept constant for all 12 tested materials. As it can be seen in Table 3 none of the polymer tribocomposites reached the stipulated lifetime of 5000 cycles (1000 m) as all of the materials failed before 1000 m sliding distance. The criterion of failure was to reach 1 mm wear depth which is the thickness of the top layer of the tribocomposites. At 1 mm wear depth the test was stopped and the performed number of cycles were defined as the lifetime of a tribocomposite. The longest lifetime, 1364 cycles (~273 m), belongs to the VE/B/PTFE/4 sample. It is the only material that performed longer than 1000 cycles. Five samples (UPE/B/POM/2, UPE/B/MoS₂/2, UPE/B/POM/4, UPE/B/MoS₂/4 and VE/B/POM/4) had extremely short lifetime with number of cycles even below 100.

Table 3 shows the total number of cycles for each material, the average static/dynamic coefficient of friction, the maximal (bulk) temperature and the measured bulk temperature at cycle 50. The maximal (bulk) temperature is the highest measured temperature in the steel counterfaces during wear tests. The highest temperature was registered at the last cycles of the tests (Figure 4). The last column of Table 3 introduces the bulk temperature after the same sliding distance (50 cycles corresponding to 10 m). As UPE/B/POM/2 and UPE/B/MoS₂/4 did not reach 50 cycles, the bulk temperatures registered at the last cycle are shown. From Table 3 it is clear that the static coefficient of friction was higher than the dynamic coefficient of friction for all tested samples, as expected. It is also shown in Table 3 that some samples reached a relatively low maximal (bulk) temperature during the wear test, which can be explained by the lower heat generation due to the lower lifetime.

Table 3. Number of cycles, static and dynamic coefficient of friction of tested tribocomposites, and the maximal (bulk) temperature of the steel counterfaces. AISI 100Cr6 steel counterface, 4 MPa contact pressure, 50 mm/s sliding speed, 100 mm stroke.

Materials	Number of cycles	Average static coefficient of friction	Average dynamic coefficient of friction	Maximal (bulk) temperature	Bulk temperature at cycle 50
	[-]	[-]	[-]	[°C]	[°C]
UPE/B/PTFE/2	156	0.53	0.50	121	65
UPE/B/POM/2	9	1.06	0.63	41	41 (at cycle 9)
UPE/B/MoS ₂ /2	58	0.86	0.74	100	94
UPE/B/PTFE/4	765	0.45	0.31	154	42
UPE/B/POM/4	54	0.75	0.66	76	73
UPE/B/MoS ₂ /4	30	0.82	0.69	67	67 (at cycle 30)
UPE/J/PTFE/2	398	0.56	0.36	144	62
UPE/J/POM/2	332	0.59	0.38	138	93
UPE/J/MoS ₂ /2	197	0.62	0.51	119	60
VE/B/PTFE/4	1364	0.30	0.22	132	38
VE/B/POM/4	64	0.62	0.51	87	81
VE/B/MoS ₂ /4	103	0.75	0.67	98	75

Figure 4 displays the curves of bulk temperature (a), (c), (e) and dynamic coefficient of friction (b), (d), (f) for PTFE/POM/MoS₂ filled tribocomposites. PTFE filled samples reached a relatively high number of cycles compared to the other tribo-fillers. Most of the other samples did not reach 100 cycles due to their failure, except UPE/J/POM/2, UPE/J/MoS₂/2 and VE/B/MoS₂/4. Independently of the material combination it is evident from Figure 4 that higher coefficient of friction resulted into higher bulk temperature. From Table 3 it can be seen that those two materials which had the lowest bulk temperature at cycle 50 reached the highest lifetime. Specifically VE/B/PTFE/4 reached 1364 cycles with a bulk temperature of 38°C at cycle 50 while UPE/B/PTFE/4 reached 765 cycles with a bulk temperature of 42°C at cycle 50. Due to

the higher temperature, the mechanical properties of the specimens decreased and the materials failed, in other words the wear depth reached the thickness of the top layer (1 mm).

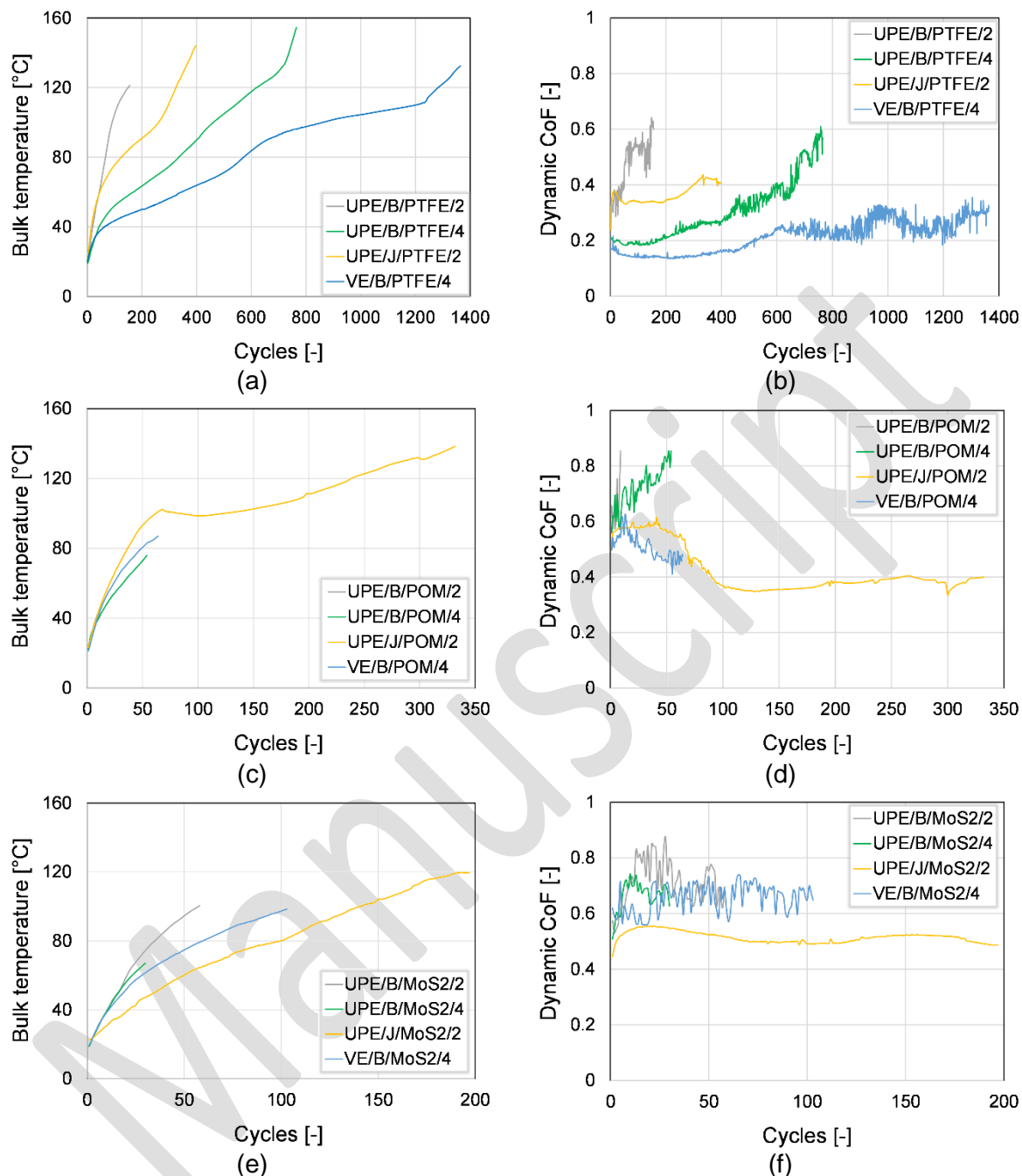


Figure 4. Bulk temperature and dynamic coefficient of friction (Dynamic CoF) curves of PTFE (a) and (b) / POM (c) and (d) / MoS₂ (e) and (f) filled tribocomposite – steel counterface pairs. AISI 100Cr6 steel counterface, 4 MPa contact pressure, 50 mm/s sliding speed, 100 mm stroke.

Figure 5 shows the worn surfaces of the tested tribocomposites. For easy understanding and comparison the maximum bulk temperature (red) is indicated at the bottom-left corner of the macrograph and the dynamic coefficient of friction (black) and total number of cycles (blue) are indicated at the top-left and top-right corner, respectively.

All materials failed due to thermal degradation and delamination which comes from the high contact temperature and from the intensive shear stress during testing. As a result of the

thermal degradation of the thermoset matrix resin, the mechanical strength and adhesion between the layers decreased and consequently the top layer was delaminated. Delamination is a typical failure method in layered composites [38]. In case of jute reinforced composites more significant delamination was observed than with basalt composites.

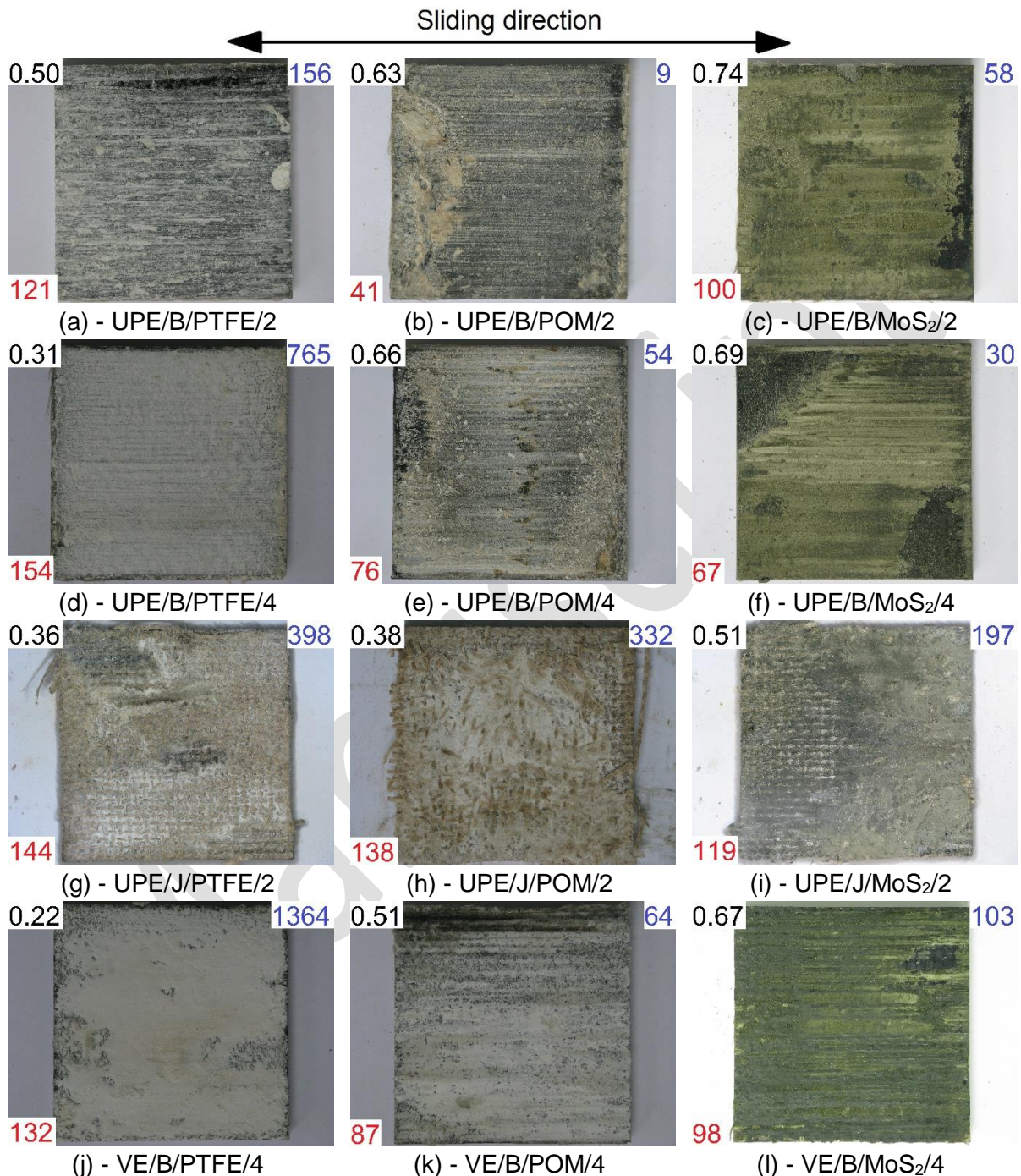


Figure 5. Macrograph of worn surfaces of the tested composites. The dynamic coefficient of friction is written by black (top-left corner), the number of cycles by blue (top-right corner) and the maximal (bulk) temperature by red (bottom-left corner). AISI 100Cr6 steel counterface, 4 MPa contact pressure, 50 mm/s sliding speed, 100 mm stroke.

Figure 6 and 7 highlight some examples of the failure mechanisms. Beside thermal degradation of the matrix, abrasion is also visible from the groove pattern along the sliding direction.

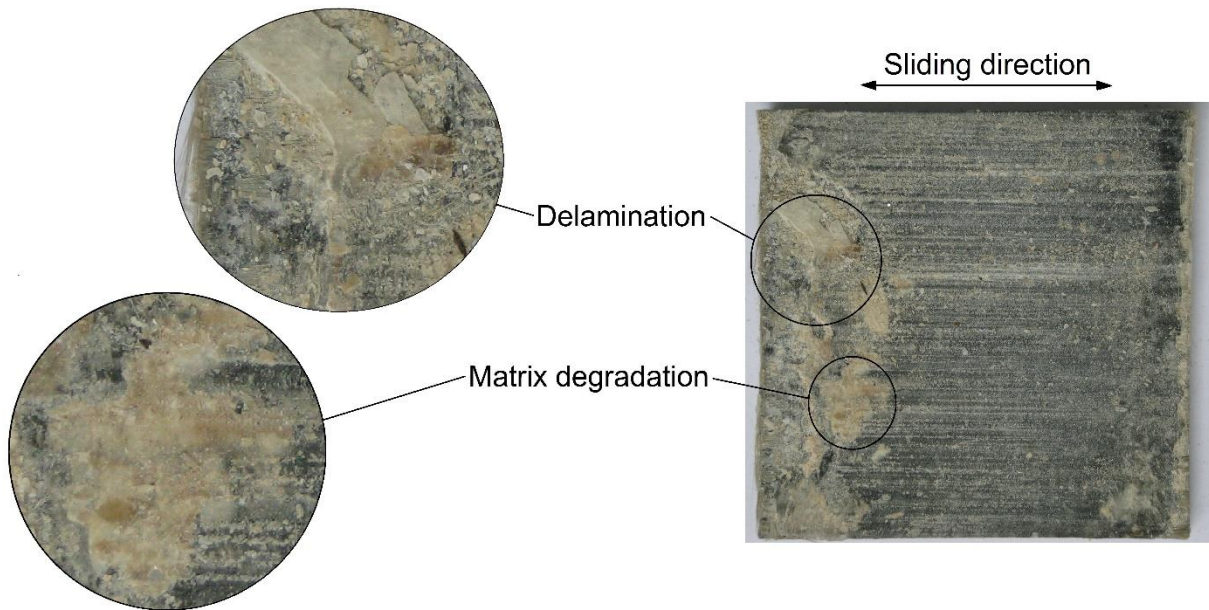


Figure 6. Failure mechanism of basalt fibre reinforced composite

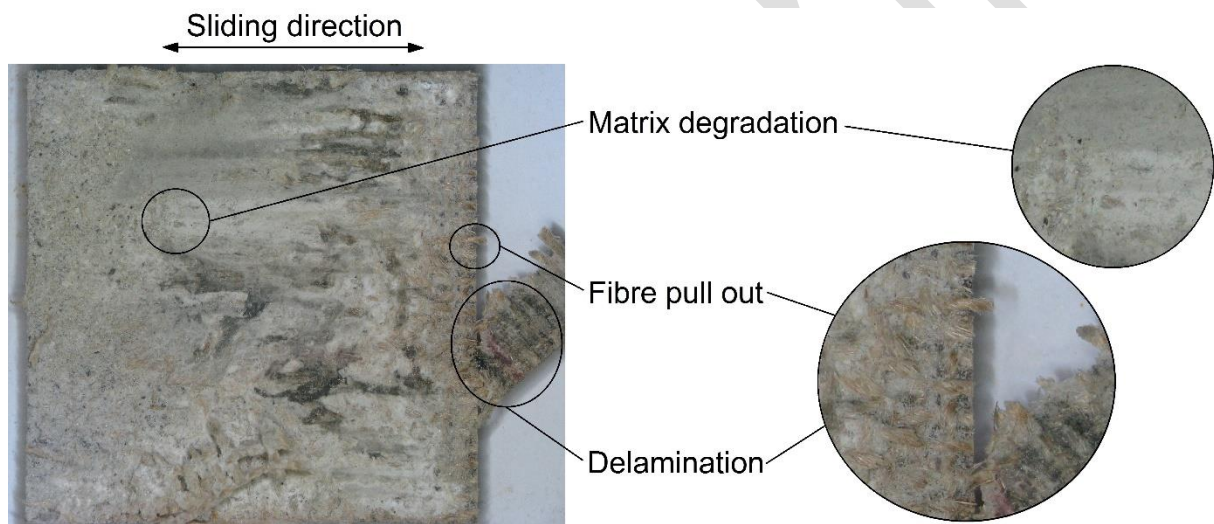


Figure 7. Failure mechanism of jute fibre reinforced composite

Figure 8 shows for all tested tribocomposites the total lifetime to failure together with the dynamic coefficient of friction. The size of the markers symbolizes the number of cycles to failure, in other words the lifetime. Unsaturated polyester based jute textile reinforced composites with 2 wt% tribo-fillers, (UPE/J/PTFE/2, UPE/J/POM/2 and UPE/J/MoS₂/2) has lower dynamic coefficient of friction than the same samples with basalt textile reinforcement (UPE/B/PTFE/2, UPE/B/POM/2 and UPE/B/MoS₂/2). Due to the lower dynamic coefficient of friction jute reinforced samples reached a longer lifetime compared to the same composites with basalt fibres despite of their lower mechanical strength (Table 2).

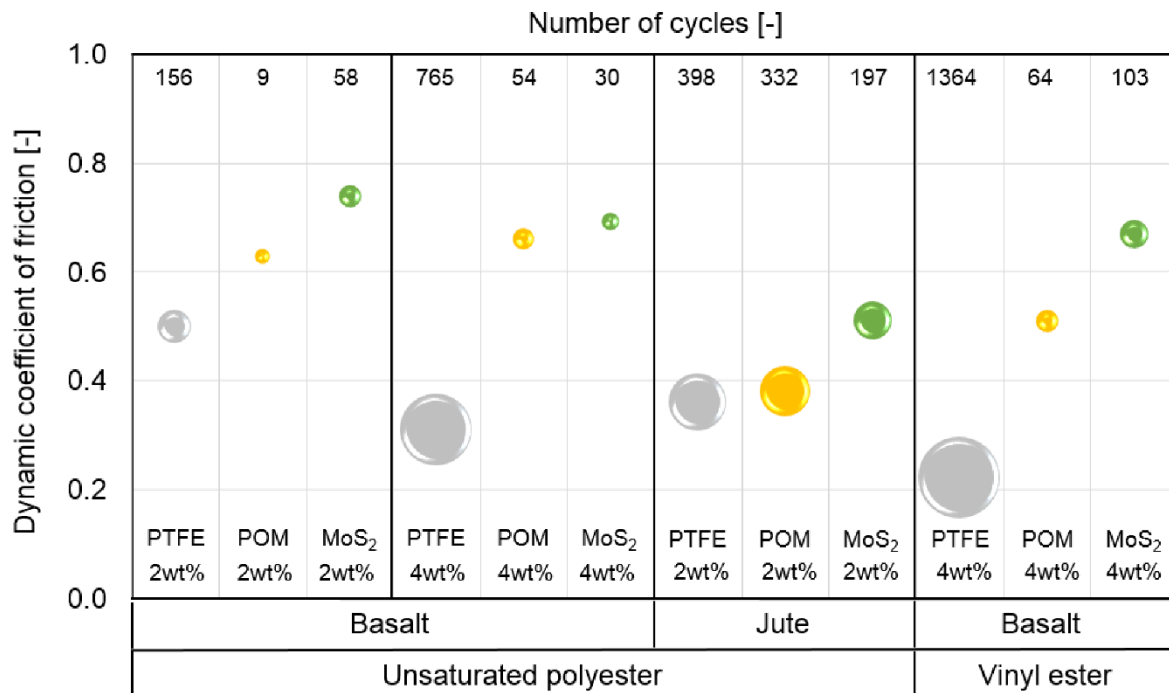


Figure 8. Dynamic coefficient of friction and lifetime of all tested polymer tribocomposites. The size of the markers correspond to the lifetime. AISI 100Cr6 steel counterface, 4 MPa contact pressure, 50 mm/s sliding speed, 100 mm stroke.

In all four groups the polymer tribocomposites with PTFE filler (UPE/B/PTFE/2, UPE/B/PTFE/4, UPE/J/PTFE/2 and VE/B/PTFE/4) have the lowest coefficient of friction and longest lifetime, which is in agreement with literature [14]. UPE/B/PTFE/4 sample had 38% lower coefficient of friction than UPE/B/PTFE/2 due to the higher PTFE content. The highest coefficient of friction values belong to samples with MoS₂ solid lubricants in all groups (UPE/B/MoS₂/2, UPE/B/MoS₂/4, UPE/J/MoS₂/2 and VE/B/MoS₂/4). From the plot it can be seen that samples with lower coefficient of friction performed relatively better in wear. Vinyl ester samples (VE/B/PTFE/4, VE/B/POM/4 and VE/B/MoS₂/4) reached longer lifetime than the same materials with unsaturated polyester matrix (UPE/B/PTFE/4, UPE/B/POM/4 and UPE/B/MoS₂/4). The better performance of vinyl ester based samples originates from the measured lower coefficient of friction and from the better mechanical properties of vinyl ester resin. The lowest coefficient of friction was reached by VE/B/PTFE/4, this value was 0.22, which is ~29% lower than UPE/B/PTFE/4 that had the second lowest coefficient of friction.

Figure 9 shows the curves of dynamic coefficient of friction and bulk temperature in UPE/B/PTFE/4 and VE/B/PTFE/4 samples. The black curve is the moving average of the dynamic coefficient of friction. It can be seen that the bulk temperature curve moves together with the dynamic coefficient of friction; the higher friction values increased the temperature, which led to thermal degradation of the matrix and simultaneously to the reduction of the mechanical properties of the composites, finally resulting into failure.

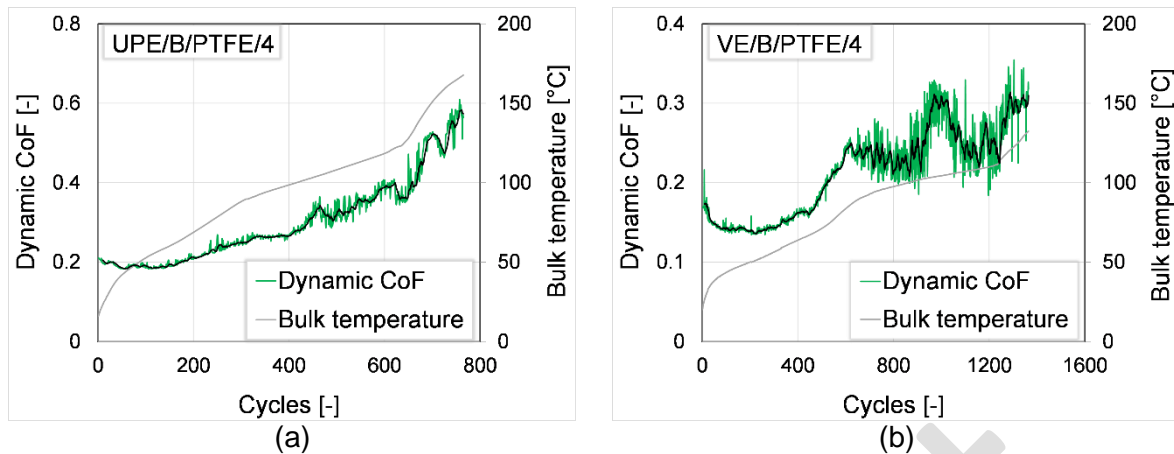


Figure 9. Dynamic coefficient of friction (Dynamic CoF) and bulk temperature of UPE/B/PTFE/4 (a) and VE/B/PTFE/4 (b) composites. AISI 100Cr6 steel counterface, 4 MPa contact pressure, 50 mm/s sliding speed, 100 mm stroke. The black curve is the moving average of the dynamic coefficient of friction with a period value of 10.

3.3. Transfer layer analysis

One of the key factors in polymer tribology is the formation of a uniform and adequate transfer layer during the wear process. To have a deeper understanding of the transfer layer, the worn steel counterfaces were investigated at both micro- and macroscale.

Figure 10 shows some macrographs of samples with different tribo-fillers (PTFE, POM, MoS₂). The transfer layer is clearly visible. Literature makes distinction between the primary and the secondary transfer layer [39]. The primary transfer layer is considered as a deposit between the asperities of the metal counterface. The secondary transfer layer is the result of a step by step deposition process, formed on top of the primary transfer layer. The white coloured primary transfer layer can be seen in (a) and (b), generated by friction of UPE/B/PTFE/2 and VE/B/POM/4 respectively. This white colour of PTFE and POM is well reflected in the transfer layer. Figure 10 (c) - UPE/B/MoS₂/4 – shows a dark background on the worn surface, which is in agreement with the black colour of MoS₂. The spatial occupancy of secondary transfer layer on the steel counter surfaces are in millimetre scale for all three tribo-fillers. The macrographs of Figure 10 also show abrasive wear scars on the steel counterfaces. These scars are caused by the removed materials and fibres of the polymer tribocomposites. It can be seen in Figure 10 that in case of PTFE (a) the abrasive wear scars are less significant than in case of POM (b) and MoS₂ (c) tribo-fillers. The less scratch marks on the counter surfaces can be attributed with the soft nature and effective self-lubricating behaviour of PTFE.

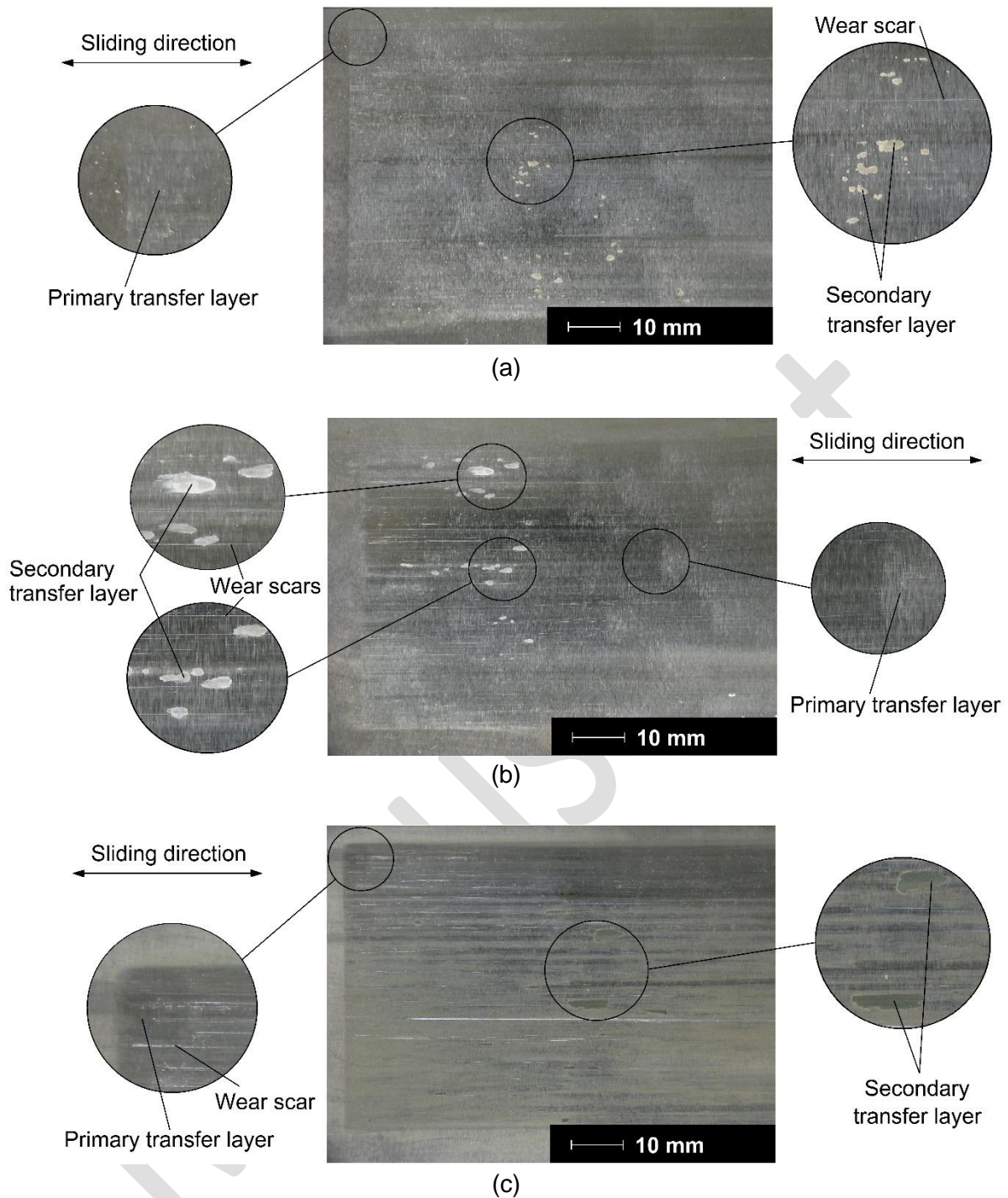


Figure 10. Macrograph of UPE/B/PTFE/2 (a), VE/B/POM/4 (b) and UPE/B/MoS₂/4 (c). AISI 100Cr6 steel counterface, 4 MPa contact pressure, 50 mm/s sliding speed, 100 mm stroke.

Figure 11 displays the micrographs of the tested steel counterfaces at x20 magnification. Each micrograph was taken at 30% intensity of Xenon illumination and exposure time of 150 μ s in order to keep control of discoloration of the contact surfaces. The micrographs show the worn surfaces with the formed transfer layer and the local wear scars. Figure 11 (a) – (f) shows areas where significant primary transfer layer was supposed. Micrograph (c) and (f) introduce a darker background caused by MoS₂ filler. These pictures also confirm the existing of a filler-rich transfer layer. Figure 11 (g) – (l) were taken from the areas with abrasive wear scars, which are parallel with the sliding direction. The perpendicular lines come from the polishing method of the steel counterfaces, previous to wear testing.

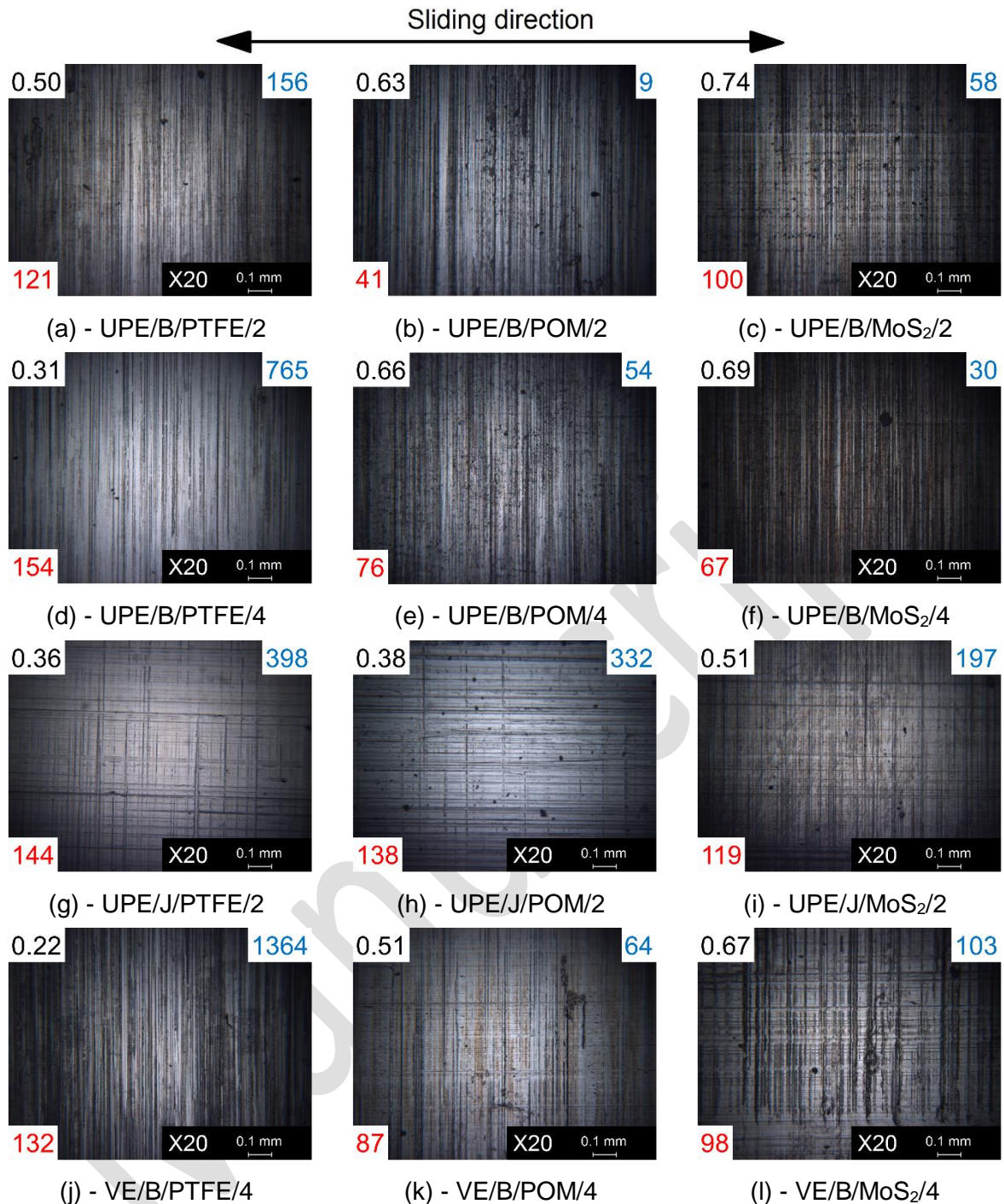


Figure 11. Micrographs of tested steel counterfaces. The dynamic coefficient of friction is written by black (top-left corner), the number of cycles by blue (top-right corner) and the maximal (bulk) temperature by red (bottom-left corner). All pictures were taken by an optical microscope with the same illumination and exposure time. AISI 100Cr6 steel counterface, 4 MPa contact pressure, 50 mm/s sliding speed, 100 mm stroke.

Table 4 and 5 introduce the Rz (peak-to-peak) and Rku (Kurtosis) surface roughness values of the steel counterfaces respectively. Rz and Rku were measured in the sliding direction (excluding the areas of scratch marks) to study the influence of the transfer layer formation. In Table 4 and 5 both unworn (before wear) and worn (after wear) surface values are given. From Table 4 can be seen that Rz decreased in all cases, but mostly the difference between the before and after wear tests was in the range of the standard deviation or close to it. In case of

jute reinforced samples, a higher difference of Rz can be seen. Rku values are also slightly reduced due to wear (Table 5) in a similar range or also close to the standard deviation. This slight difference in Rz and Rku values between worn and unworn steel surfaces indicates that the formed transfer layer on the steel surface did not influence the original surface pattern significantly (Figure 11 (a)-(f)).

Table 4. Surface roughness values (Rz) of the tested steel counterfaces before (unworn surface) and after wear (worn surface) in sliding direction. AISI 100Cr6 steel counterface, 4 MPa contact pressure, 50 mm/s sliding speed, 100 mm stroke.

Materials	Number of cycles	Rz – unworn surface		Rz – worn surface		ΔR_z
		Average	Standard deviation	Average	Standard deviation	
	[-]	[μm]	[μm]	[μm]	[μm]	[μm]
UPE/B/PTFE/2	156	1.037	0.134	0.823	0.037	0.214
UPE/B/POM/2	9	1.564	0.252	1.411	0.059	0.153
UPE/B/MoS ₂ /2	58	1.533	0.150	1.364	0.126	0.169
UPE/B/PTFE/4	765	1.091	0.132	0.925	0.096	0.166
UPE/B/POM/4	54	1.020	0.133	0.958	0.044	0.062
UPE/B/MoS ₂ /4	30	1.533	0.287	1.475	0.294	0.058
UPE/J/PTFE/2	398	0.865	0.083	0.386	0.062	0.479
UPE/J/POM/2	332	0.886	0.125	0.459	0.053	0.427
UPE/J/MoS ₂ /2	197	0.811	0.085	0.224	0.078	0.587
VE/B/PTFE/4	1367	1.449	0.118	1.357	0.098	0.092
VE/B/POM/4	64	1.774	0.263	1.493	0.227	0.281
VE/B/MoS ₂ /4	103	1.807	0.339	1.644	0.207	0.163

Table 5. Surface roughness values (Rku) of the tested steel counterfaces before (unworn surface) and after wear (worn surface) in sliding direction. AISI 100Cr6 steel counterface, 4 MPa contact pressure, 50 mm/s sliding speed, 100 mm stroke.

Materials	Number of cycles	Rku – unworn surface		Rku – worn surface		ΔR_{ku}
		Average	Standard deviation	Average	Standard deviation	
	[-]	[μm]	[μm]	[μm]	[μm]	[μm]
UPE/B/PTFE/2	156	3.901	0.255	3.089	0.355	0.812
UPE/B/POM/2	9	3.322	0.455	3.343	0.394	-0.021
UPE/B/MoS ₂ /2	58	3.735	0.329	3.199	0.124	0.536
UPE/B/PTFE/4	765	4.330	0.744	3.831	0.559	0.499
UPE/B/POM/4	54	4.259	0.529	3.411	0.263	0.848
UPE/B/MoS ₂ /4	30	3.198	0.349	3.090	0.109	0.108
UPE/J/PTFE/2	398	3.205	0.493	2.960	0.314	0.245
UPE/J/POM/2	332	3.181	0.210	2.976	0.435	0.205
UPE/J/MoS ₂ /2	197	3.351	0.714	3.371	0.879	-0.02
VE/B/PTFE/4	1367	3.836	0.280	3.702	0.420	0.134
VE/B/POM/4	64	3.535	0.633	3.476	0.290	0.059
VE/B/MoS ₂ /4	103	3.263	0.432	3.184	0.455	0.079

4. Conclusions

In this research work PTFE/POM/MoS₂ filled tribocomposites were investigated. From the results of this characterisation, the following conclusions can be drawn:

- 1 Focusing on the tensile and flexural strength PTFE, POM and MoS₂ tribo-fillers show the same mechanical performance in the investigated tribocomposites. On the other hand in tribological viewpoint significant differences were registered. Semi-crystalline thermoplastic tribo-fillers as PTFE and POM reached a lower coefficient of friction than the lamellar structured MoS₂.
- 2 PTFE filled samples showed the lowest coefficient of friction which comes from the excellent lubricating behaviour of PTFE. Due to the low coefficient of friction the frictional heating was also moderated and consequently PTFE filled tribocomposites had the longest lifetime.
- 3 Specimens with vinyl ester matrix had higher lifetime compared to the same composites based on unsaturated polyester. This can be attributed to the advanced tensile and flexural strength of vinyl ester composites. The longest lifetime was found for VE/B/PTFE/4 with 1364 cycles.
- 4 The failure method for all tested tribocomposites was matrix thermal degradation and delamination. This phenomenon comes from the intensive shear stress during wear process and from the high frictional heating which degraded the thermoset matrices decreasing their mechanical properties.
- 5 Transfer layer formation generated from PTFE/POM/MoS₂ tribo-fillers was clearly observed for steel counterfaces both in micro- and macrographs. Primary and secondary transfer layer were registered. The transfer layer formation is beneficial as it enables improved coefficient of friction and increased lifetime. Abrasive wear scars were also observed on the steel counterfaces but in case of PTFE solid lubricant it is less significant. The formed transfer layer did not change the dominating surface characteristic of the steel counter surfaces.

Based on the results of this research work finding the optimal tribo-filler ratio and the hybridization of this composite materials could be considered to further improve the wear properties.

5. Acknowledgement

This investigation was supported and funded by Fonds Wetenschappelijk Onderzoek – Vlaanderen (FWO) 12S1918N. This research was performed under a cooperative effort between Ghent University (Belgium) and Budapest University of Technology and Economics (Hungary). Laboratory Soete acknowledges the material support received from Centre for Composite Materials, Department of Mechanical Engineering, Kalasalingam University (Krishnankoil-626126, Tamilnadu, India). The authors are grateful to Sam Nowé and Wouter Ost for their support on experimental activities.

6. References

- [1] J.M. Thorp, Friction of some commercial polymer-based bearing materials against steel, *Tribol. Int.* (1982) 69-74.
- [2] K. Mao, W. Li, C.J. Hooke, D. Walton, Friction and wear behaviour of acetal and nylon gears, *Wear* 267 (2009) 639-645.

- [3] B.B. Jia, T.S. Li, X.J. Liu, P.H. Cong, Tribological behaviours of several polymer–polymer sliding combinations under dry friction and oil-lubricated conditions, *Wear* 262 (2007) 1353-1359.
- [4] H. Unal, U. Sen, A. Mimaroglu, Dry sliding wear characteristics of some industrial polymers against steel counterface, *Tribol. Int.* 37 (2004) 727-732.
- [5] L. Lin, X.Q. Pei, R. Bennewitz, A.K. Schlarb, Friction and wear of PEEK in continuous sliding and unidirectional scratch tests, *Tribol. Int.* 122 (2018) 108-113.
- [6] J.R. Vail, B.A. Krick, K.R. Marchman, W.G. Sawyer, Polytetrafluoroethylene (PTFE) fiber reinforced polyetheretherketone (PEEK) composites, *Wear* 270 (2011) 737-741.
- [7] A.C. Greco, R. Erck, O. Ajayi, G. Fenske, Effect of reinforcement morphology on high-speed sliding friction and wear of PEEK polymers, *Wear* 271 (2011) 2222-2229.
- [8] A. Pogacnik, M. Kalin, Parameters influencing the running-in and long-term tribological behaviour of polyamide (PA) against polyacetal (POM) and steel, *Wear* 290-291 (2012) 140-148.
- [9] J. Sukumaran, J. De Pauw, P.D. Neis, L.F. Tóth, P. De Baets, Revisiting polymer tribology for heavy duty application, *Wear* 376-377 (2017) 1321-1332.
- [10] P.H. Pinchbeck, A review of plastic bearings, *Wear* 5 (1962) 85-113.
- [11] A. Imani, H. Zhang, M. Owais, J. Zhao, P. Chu, J. Yang, Z. Zhang, Wear and friction of epoxy based nanocomposites with silica nanoparticles and wax-containing microcapsules, *Compos. Part A - Appl. S.* 107 (2018) 607-615.
- [12] Z. Rymuza, Tribology of Polymers, *Arch. Civ. Mech. Eng.* 7 (2007) 177-184.
- [13] B. Chen, X. Li, Y. Jia, X. Li, J. Yang, F. Yan, C. Li, MoS₂ nanosheets-decorated carbon fiber hybrid for improving the friction and wear properties of polyimide composite, *Compos. Part A - Appl. S.* 109 (2018) 232-238.
- [14] K.D. Dearn, T.J. Hoskins, D.G. Petrov, S.C. Reynolds, R. Banks, Applications of dry film lubricants for polymer gears, *Wear* 298-299 (2013) 99-108.
- [15] U. Nirmal, J. Hashim, M.M.H.M. Ahmad, A review on tribological performance of natural fibre polymeric composites, *Tribol. Int.* 83 (2015) 77-104.
- [16] S. Zhou, J. Wang, S. Wang, X. Ma, J. Huang, G. Zhao, Y. Liu, Facile preparation of multiscale graphene-basalt fiber reinforcements and their enhanced mechanical and tribological properties for polyamide 6 composites, *Mater. Chem. Phys.* 217 (2018) 315-322.
- [17] C.R. Mahesha, Shivarudraiah, N. Mohan, M. Rajesh, Role of nanofillers on mechanical and dry sliding wear behavior of basalt- epoxy nanocomposites, *Mater. Today - Proc.* 4 (2017) 8192-8199.
- [18] M.R. Bambach, Compression strength of natural fibre composite plates and sections of flax, jute and hemp, *Thin Wall. Struct.* 119 (2017) 103-113.
- [19] A.L. Duigou, A. Kervoelen, A.L. Grand, M. Nardin, C. Baley, Interfacial properties of flax fibre–epoxy resin systems: Existence of a complex interphase, *Compos. Sci. Technol.* 100 (2014) 152-157.
- [20] Y. Li, L. Xie, H. Ma, Permeability and mechanical properties of plant fiber reinforced hybrid composites, *Mater. Des.* 86 (2015) 313-320.
- [21] M. Afroz, I. Patnaikuni, S. Venkatesan, Chemical durability and performance of modified basalt fiber in concrete medium, *Constr. Build. Mater.* 154 (2017) 191-203.
- [22] V. Fiore, T. Scalici, G. Di Bella, A. Valenza, A review on basalt fibre and its composites, *Compos. Part B - Eng.* 74 (2015) 74-94.
- [23] T. Deák, T. Czigány, Chemical Composition and Mechanical Properties of Basalt and Glass Fibers: A Comparison, *Text. Res. J.* 79 (2009) 645-651.

- [24] T. Czigány, J. Vad, K. Pölöskei, Basalt fiber as a reinforcement of polymer composites, *Period. Polytech. Mech.* 49 (2005) 3-14.
- [25] M.F. Pucci, M.C. Seghini, P.J. Liotier, F. Sarasini, J. Tirilló, S. Drapier, Surface characterisation and wetting properties of single basalt fibres, *Compos. Part B - Eng.* 109 (2017) 72-81.
- [26] T. Tábi, A.Z. Égerházi, P. Tamás, T. Czigány, J.G. Kovács, Investigation of injection moulded poly(lactic acid) reinforced with long basalt fibres, *Compos. Part A - Appl. S.* 64 (2014) 99-106.
- [27] G. Sun, S. Tong, D. Chen, Z. Gong, Q. Li, Mechanical properties of hybrid composites reinforced by carbon and basalt fibers, *Int. J. Mech. Sci.* 148 (2018) 636-651.
- [28] Q. Hu, P. Wang, J. Jiang, H. Pan, D.W. Gao, Column adsorption of aniline by a surface modified jute fiber and its regeneration property, *J. Environ. Chem. Eng.* 4 (2016) 2243-2249.
- [29] O. Faruk, A.K. Bledzki, H.P. Fink, M. Sain, Biocomposites reinforced with natural fibers: 2000-2010, *Prog. Polym. Sci.* 37 (2012) 1552-1596.
- [30] E. Omrani, P.L. Menezes, P.K. Rohatgi, State of the art on tribological behavior of polymer matrix composites reinforced with natural fibers in the green materials world, *Eng. Sci. Technol. Int. J.* 19 (2016) 717-736.
- [31] G.M. Zakriya, G. Ramakrishnan, Insulation and mechanical properties of jute and hollow conjugated polyester reinforced nonwoven composite, *Energ. Buildings* 158 (2018) 1544-1552.
- [32] P.V. Bansod, A.R. Mohanty, Inverse acoustical characterization of natural jute sound absorbing material by the particle swarm optimization method, *Appl. Acoust.* 112 (2016) 41-52.
- [33] M. Ramesh, K. Palanikumar, K.H. Reddy, Plant fibre based bio-composites: Sustainable and renewable green materials, *Renew. Sust. Energ. Rev.* 79 (2017) 558-584.
- [34] C.W. Zhang, F.Y. Li, J.F. Li, Y.L. Li, J. Xu, Q. Xie, S. Chen, A.F. Guo, Novel treatments for compatibility of plant fiber and starch by forming new hydrogen bonds, *J. Clean. Prod.* 185 (2018) 357-365.
- [35] K. Subramanian, R. Nagarajan, P. De Baets, S. Subramaniam, W. Thangiah, J. Sukumaran, Eco-friendly mono-layered PTFE blended polymer composites for dry sliding tribo – systems, *Tribol. Int.* 102 (2016) 569-579.
- [36] J.T. Shen, M. Top, Y.T. Pei, J.T.M. De Hosson, Wear and friction performance of PTFE filled epoxy composites with a high concentration of SiO₂ particles, *Wear* 322-323 (2015) 171-180.
- [37] V. Rodriguez, J. Sukumaran, A.K. Schlarb, P. De Baets, Reciprocating sliding wear behaviour of PEEK-based hybrid composites, *Wear* 362-363 (2016) 161-169.
- [38] M.R. Hosseini, F. Taheri-Behrooz, M. Salamat-talab, Mode I interlaminar fracture toughness of woven glass/epoxy composites with mat layers at delamination interface, *Polym. Test.* 78 (2019) 105943.
- [39] J. Sukumaran, Vision Assisted Tribography of Rolling-Sliding Contact of Polymer-Steel Pairs, PhD dissertation, Ghent University, Belgium, 2014.